Solid State $^{31}P/^{27}Al$ and $^{31}P/^{23}Na$ MAS NMR Dipolar Dephasing Investigations of Connectivity in Sodium Aluminophosphate Glasses[†]

David P. Lang,[1*] Todd M. Alam[1] and Denise N. Bencoe[2]

[1] Sandia National Laboratories, Organic Materials Department, Albuquerque, NM 87185-1407 USA.
[2] Sandia National Laboratories, Materials Processing Department, Advanced Materials Laboratory, 1001 University Blvd. SE., Albuquerque, NM 87106 USA.

Solid state $^{31}P/^{27}Al$ and $^{31}P/^{23}Na$ MAS NMR dipolar dephasing experiments have been used to investigate the spatial distribution of aluminum and sodium cations with respect to the phosphate backbone for a series of sodium aluminophosphate glasses, $xAl_2O_3 \cdot 50Na_2O \cdot (50\text{-}x)P_2O_5$ ($0 \leq x \leq 17.5$). From the $^{31}P/^{27}Al$ and $^{31}P/^{23}Na$ connectivity data gathered, information about the medium range order in these glasses is obtained. The expanded connectivity data allows for better identification and interpretation of the new resonances observed in the ^{31}P MAS NMR spectra with the addition of alumina. The results of the dipolar dephasing experiments show that the sodium-phosphate distribution remains relatively unchanged for the glass series, and that the addition of aluminum occurs primarily through the depolymerization of the phosphate tetrahedral backbone.

[†] Sandia is a multiprogram laboratory operated by Sandia Corporation, a Lockheed Martin Company, for the United States Department of Energy under Contract DE-AC04-94AL85000.
[*] Author to whom correspondence should be addressed: dplang@sandia.gov

DISCLAIMER

Introduction

The continued development of phosphate glasses for a variety of technologically important applications including glass-to-metal seals[1,2] and laser hosts[3,4] can be impeded by the low durability often associated with these materials. The addition of alumina to simple phosphate glasses, however, has been shown to have a dramatic impact on their dissolution durability. For example, more than a five-order reduction in the dissolution rate has been observed with a 15 molar percent (mole%) addition of Al_2O_3 to a sodium phosphate glass.[5] Thus, an understanding of the basic structural changes that occur with the addition of alumina is important for the rational design of new glasses for specific applications.

In its crystalline form, P_2O_5 has a polymerized structure consisting of phosphorus tetrahedra with three bridging oxygen bonds (BO) and one terminal non-bridging oxygen bond (NBO).[6,7] Depolymerization of a glass network occurs when alkali-metal or alkaline-earth oxides (such as Na_2O, Li_2O, CaO) are added to the glass melt.[6,8] For example, when Na_2O is added depolymerization results in the replacement of P-O-P linkages with the much weaker P-O-Na bonds.[5,9] Addition of aluminum oxide , Al_2O_3, to the melt also affects the glass network, but changes in the physical properties often imply that the structural polymerization has increased rather than decreased.[5,10]

Magic-angle spinning (MAS) nuclear magnetic resonance (NMR) spectroscopy has proven to be a valuable technique for probing the structural changes occurring in the evolution of binary or ternary phosphate glass systems.[11-13] Using one-dimensional (1D) MAS NMR differing local chemical environments for phosphorus and the modifier cations can often be discriminated and quantified. This short-range structural information

allows for a better understanding of the physical properties of the glass, but gives little or no information about their structural connectivity or medium range order (MRO). Structural variations in the MRO may also play a significant role in controlling the physical properties of a glass.

NMR techniques that utilize through-space dipole-dipole coupling between nuclei allow such spatial connectivity to be established. The two-dimensional radio-frequency dipolar recoupling (2D RFDR) experiment is one method for reintroducing magnetization exchange between homonuclear dipolar coupled spins, and has been used to probe the MRO between phosphorous nuclei.[14-17] Homonuclear multiple-quantum (MQ) experiments, which are more resolved than the RFDR spectra, have also been used to study the MRO in crystalline and glassy phosphate systems.[7,17-21] While the ^{31}P-^{31}P homonuclear magnetization exchange techniques provide information about the structural backbone of the phosphate systems, they do not yield any information about the connectivity of phosphorus and the other network constituents, e.g., ^{23}Na or ^{27}Al to ^{31}P. Such heteronuclear dipolar analysis is often complicated by the fact that the other constituents are quadrupolar nuclei ($I > ½$), and the spin dynamics and magnitude of the quadrupolar interaction often requires that unique NMR techniques be used.

Recently, several MAS-based NMR techniques have been developed that utilize the heteronuclear dipolar coupling between quadrupolar and spin-1/2 nuclei to ascertain connectivity and spatial interaction information. These include Cross Polarization (CP) involving quadrupolar nuclei,[22-24] Rotational Echo DOuble Resonance (REDOR),[25-27] Transferred Echo DOuble Resonance (TEDOR),[27,28] Dipolar Dephasing and TRAsfer of Populations DOuble Resonance (TRAPDOR),[29-32] Rotational Echo Adiabatic

Passage DOuble Resonance (REAPDOR)[33] and Dipolar Exchange Assisted Recoupling (DEAR) experiments.[34] Many of these techniques have thus been employed and combined to acquire structural information in mixed quadrupolar, spin-1/2 nuclei systems including glasses,[17,35-42] zeolites[27,31,32,43,44] and aluminophosphates.[45-51]

In this investigation we report the $^{31}P/^{27}Al$ and $^{31}P/^{23}Na$ NMR dipolar dephasing results for the sodium aluminophosphate glass series, $xAl_2O_3 \cdot 50Na_2O \cdot (50-x)P_2O_5$ ($0 \leq x \leq 17.5$). Previously, Brow and Kirkpatrick[9] reported the 1D ^{31}P and ^{27}Al MAS NMR results for the glass series $xAl_2O_3 \cdot 50Na_2O \cdot (50-x)P_2O_5$ ($0 \leq x \leq 20$). Recently, Egan et al. also analyzed three glasses within this series, x = 7.5, 10 and 12.5 mole% alumina, using a 2D heteronuclear CP correlation experiment to observe changes in $^{31}P/^{27}Al$ connectivity as the glass transforms from a metaphosphate to pyrophosphate composition.[41] In these investigations only a single isotropic resonance in the 1D ^{31}P MAS spectra was delineated even though asymmetric resonances and shoulder feature were clearly observed. Subsequent NMR experiments within our laboratory have revealed that there are actually several new resolvable resonances that appear with the addition of alumina. The results of the combined $^{31}P/^{27}Al$ and $^{31}P/^{23}Na$ dipolar dephasing experiments described here allow the assignment of these new ^{31}P NMR resonances, along with a discussion of the role of sodium and alumina in the MRO development for these glasses.

Experimental Procedures

Sample Preparation. Eight sodium aluminophosphate (NAP) glasses were prepared using a metaphosphate base glass ($NaPO_3$), αAl_2O_3(99.99%) and sodium carbonate (Na_2CO_3)(assay 99.6%).[5] The metaphosphate base glass was prepared using technical

grade crystalline sodium hexametaphosphate $(NaPO_3)_6$, melted in a platinum crucible at 900°C for one hour. O_2 was bubbled in the melt (through a SiO_2 tube) for half the time, and above the melt for the rest of the time. Quenching between two stainless steel plates produced thin pieces of glass which were then ground up with a steel mortar/pestle and put through a 1.18mm sieve. All eight compositions were prepared with the same raw materials, melted in platinum crucibles, quenched in heated stainless steel molds, annealed for one hour at ~30-40° above T_g, slow-furnace cooled to room temperature, and stored in a dessicator. Glass compositions vary with 2.5 mole% increases in αAl_2O_3. Individual glasses will be identified by their batch composition. For example, the label (50-5-45) for a NAP glass refers to the composition (in mole%) $50Na_2O{\cdot}5Al_2O_3{\cdot}45P_2O_5$. A Differential Scanning Calorimeter was used to measure the onset of glass transition (T_g) and glass crystallization (T_x) for each glass in the series.

NMR Experiments. All NMR spectra were collected on a Bruker AMX400 spectrometer modified to include a third, linearly amplified, radio frequency channel. The 1D MAS NMR spectra of ^{27}Al and ^{31}P nuclei were collected using a 4 mm MAS broadband triple resonance probe and a spinning speed of 10 kHz. Spectra of aluminum were acquired at 104.271 MHz using a 4 μs π/2 pulse, 4096 signal averages, and a 0.5 second recycle delay. Spectra of phosphorus were acquired at 161.987 MHz using a 14.7 μs π/2 pulse, 32 to 512 signal averages, and a recycle delay of 120 seconds. As the samples studied are anhydrous, no ^1H decoupling was applied. The ^{27}Al and ^{31}P NMR shifts are reported using the δ scale, with positive values being downfield, and are referenced to 1M $Al(OH_2)_6^{3+}$ (δ = 0.0 ppm) and $(NH_4)H_2PO_4$ (δ = 0.8 ppm with respect to 85% H_3PO_4), respectively.

Dipolar-dephasing difference experiments (see Figure 1) were used to measure the heteronuclear dipolar interactions between the I (^{31}P) and S spins (^{27}Al or ^{23}Na) within the glass. This information was acquired by measuring the difference of the spin echo of the I nuclei obtained with and without irradiation of the S nuclei during part of the pulse sequence.[29,30,32] The continuous irradiation of the S nuclei during *n* rotor periods modifies the Zeeman population levels of the S spin, which in turn affects the magnetization of the ^{31}P nuclei dipolar coupled to it. This interference thus alters the refocusing of the ^{31}P spin echo in the pulse sequence. The dephasing difference spectrum, ΔS, was obtained by subtracting the Fourier transformed spectra of the two experiments with and without decoupling. The dipolar dephasing experiments were performed using a 4 mm MAS broadband triple resonance probe with sample rotation of 10 kHz. A 162 ± 10 MHz bandpass filter utilized on the ^{31}P channel, and a 102 ± 10 MHz bandpass filter on the ^{23}Na (or ^{27}Al) channel. NMR resonance frequencies were 161.987 MHz for ^{31}P, 104.271 MHz for ^{27}Al and 105.849 MHz for ^{23}Na. The ^{31}P $\pi/2$ pulse was 17.5 μs, corresponding to a rf field strength of 14.3 kHz, and was applied with minimal offset. To minimize variations in experimental conditions, and eliminate spectrometer artifacts, the ^{27}Al or ^{23}Na decoupling pulse on the S nuclei was triggered in both experiments with minimal offset,[32] from very high (120dB) attenuation for no S decoupling, to low (12dB) for maximum S decoupling. As the ^{31}P $\pi/2$ and π pulses were synchronized with the rotor period, the length of the decoupling pulse varied from 4 to 100 rotor cycles (0.4 to 10 ms). At higher rf amplitudes (lower attenuation values) the effects of the dephasing difference spectrum are maximized. Finally, as the difference between the resonance frequencies of ^{27}Al and ^{23}Na is rather small (1.6 MHz for our

magnet) the possibility of the irradiation of ^{27}Al affecting ^{23}Na, or vice versa, was investigated. A trial $^{31}P/^{27}Al$ dipolar dephasing experiment performed on the 50-0-50 glass, which contains no aluminum, and involving irradiation of ^{27}Al during 30 rotor cycles, yielded a null difference, ΔS, spectrum as expected. Similarly, a trial $^{31}P/^{23}Na$ dipolar dephasing experiment performed on $AlPO_4$, which contains no sodium, showed no dephasing difference effect, either. These null experiments clearly demonstrate that the observed dephasing effects are not due to low frequency isolation between the sodium and aluminum channels of the probe, but result directly from heteronuclear dipolar interactions.

Results

All eight sodium aluminophosphate glasses were examined by a variety of NMR techniques. One-dimensional ^{31}P and ^{27}Al MAS NMR allow observation of the systematic changes occurring in the structure of the glass with increasing mole% alumina. Information about the proximity of phosphorus and aluminum, or phosphorus and sodium, was obtained using $^{31}P/^{27}Al$ and $^{31}P/^{23}Na$ dipolar dephasing experiments, respectively. We will designate the aluminophosphate structures using a $Q^n(m\text{Al})$ notation, where n is the number of P next-nearest-neighbor (NNN) per P tetrahedron and m is the number of Al NNN per P. Thus, the crystalline compound $Al(PO_3)_3$ is described by a $Q^2(2\text{Al})$ phosphate structure,[52] $AlPO_4$ has a $Q^0(4\text{Al})$ structure,[53] and $KAlP_2O_7$ has a $Q^1(3\text{Al})$ structure.[54] Note that this notation makes no distinction as to the coordination number of aluminum; as we are not able to distinguish the aluminum coordination

number in our dipolar dephasing experiments, we will use this notation for all subsequent discussion.

^{31}P MAS NMR. The ^{31}P MAS NMR spectra of the NAP glasses are shown in Figure 2, with the evolution of the glass system as the mole% alumina increases being readily seen. Due to site overlap and inhomogeneous broadening, deconvolution of the spectrum into individual sites is difficult. However, using the procedures of Herzfeld and Berger,[55] attempts were made to deconvolute the entire MAS NMR sideband manifold of each spectrum and best 'fit' them to unique phosphorus environments. Changes in the ^{31}P isotropic chemical shift values can be understood from the known relationships between the NNN bonding environments of P and comparison to the ^{31}P chemical shifts of model phosphate and aluminophosphate structures.[9] The ^{31}P isotropic chemical shift value for each site and its fractional population as a function of the mole% alumina are listed in Table 1. The general trend for the weighted-average of the ^{31}P chemical shift values reported here are consistent with those reported by Brow et al.[9]

The ^{31}P NMR spectrum of the sodium metaphosphate base glass, 50-0-50, displays the presence of $Q^2(0Al)$ (two bridging POP bonds per P) and $Q^1(0Al)$ (one bridging POP bond per P) phosphorus tetrahedral environments (see Figure 2). Two structural designs consistent with such a spectrum are of a linear chain of $Q^2(0Al)$ species terminated by $Q^1(0\ Al)$ end groups, or of cyclic structures of $Q^2(0Al)$ species existing concomitantly with a concentration of $Q^1(0Al)$ diphosphate species. A radio-frequency dipolar recoupling experiment (RFDR) performed on this sample (Figure not shown) supports the first scenario, as prominent cross peaks existing within the spectrum indicate strong dipolar coupling between the $Q^2(0Al)$ and $Q^1(0Al)$ species; this is consistent with similar

RFDR investigations of lithium-phosphate glasses.[16] Such dipolar coupling would not exist if the species were isolated from one another, as would be the case in the second structural scenario.[19] The existence of a significant $Q^1(0Al)$ fraction within the 50-0-50 spectrum indicates that the composition of our sodium metaphosphate base glass is modifier-rich, Na/P > 1. Using equations developed by Van Wazer,[6,12] the nominal molar composition of our base glass is calculated at 52.4-0-47.6 rather than the assumed 50-0-50. The loss of P_2O_5 occurs during the glass preparation process when high melting temperatures are used.[5,56] This base glass was used in the preparation of all the remaining compositions.

Addition of αAl_2O_3 to the $NaPO_3$ base glass results in the formation of two new phosphorus environments, a prominent one with a ^{31}P chemical shift at ~ –7 ppm and a smaller resonance at ~ –14 ppm. The creation of these environments reduces the fractional population of $Q^2(0Al)$ tetrahedral species, but diminishes the $Q^1(0Al)$ species only negligibly until the mole% alumina is ≥ 10 (see Figure 2 and Table 1). For example, the ^{31}P spectrum of the 50-2.5-47.5 glass has a new isotropic phosphorus resonance at –7.1 ppm, while the $Q^2(0Al)$ resonance has shifted downfield by ~ 0.6 ppm and left the chemical shift and concentration of the $Q^1(0Al)$ resonance nearly unchanged. The new phosphorus resonance is attributed to the replacement of $Q^2(0Al)$ POP linkages with $Q^1(mAl)$ m = 1,2 POAl linkages.[9,57] As the mole% alumina increases, so too does the extent of the conversion of $Q^2(0Al)$ species into $Q^1(mAl)$ species. For example, in the 50-7.5-42.5 glass the $Q^2(0Al)$ species are no longer resolved; rather, both the $Q^2(0Al)$ and the $Q^1(0Al)$ resonance, to a lesser extent, exist as shoulder features on the upfield and downfield sides of the $Q^1(mAl)$ peak(s), respectively. The conversion of the $Q^2(0Al)$

species to $Q^1(m\text{Al})$ m = 1,2 species continues through 10 mole% alumina, at which time their conversion appears complete. The ^{31}P spectrum of the 50-10-40 glass consists of a broad asymmetric, upfield tailing $Q^1(m\text{Al})$ resonance, and a smaller downfield resonance. The downfield shoulder is due to a remaining fraction of $Q^1(0\text{Al})$ end species. Additional aluminum further depolymerizes the glass, reduces the shielding on the phosphorus sites, and results in the formation of alumino-orthophosphate, $Q^0(m\text{Al})$, species. In the 50-12.5-37.5 glass, $Q^1(0\text{Al})$ is no longer the dominant resonance downfield; rather, the fully depolymerized alumino-orthophosphate species, $Q^0(2\text{Al})$ resonance at –2.8 ppm and $Q^0(1\text{Al})$ specie at 6.3 ppm are now present.[9,58] In the 50-15-35 and 50-17.5-32.5 glasses all of the $Q^1(1\text{Al})$ species, and a majority of the $Q^1(m\text{Al})$ species, have undergone full depolymerization (see Table 1) forming $Q^0(m\text{Al})$ species. Changes in the phosphorus spectra coincide with those occurring in the ^{27}Al MAS NMR spectra, and will be discussed, below.

^{27}Al MAS NMR. The results of the one-dimensional ^{27}Al MAS NMR experiments of the NAP glasses are shown in Figures 3, 4 and Table 2. All the NAP glasses have some fraction of four-coordinated, Al(4), five-coordinated Al(5) and six-coordinated Al(6) aluminum. The value of the chemical shift and relative peak area of each environment for all the NAP glasses studied are given in Table 2, and are consistent with those of Brow et al.[9] Note that the values listed in Table 2 do not take into account the quadrupolar effects of the aluminum nuclei. These effects will shift a resonance from its true isotropic value and may result in a loss of signal intensity, introducing a small error in the measured coordination percentages. However, as the most important parameter for this study is

variation in the coordination of Al as the mole% alumina changes, the error introduced by the quadrupolar effects are small.

The dominant aluminum coordination is Al(6) at $x \leq 7.5$ mole% αAl_2O_3 (see Figure 3). For the 50-2.5-47.5 glass the ratio of aluminum environments is ca. 86% Al(6), 10% Al(5) and 4% Al(4). At higher mole% αAl_2O_3, the preferred coordination changes dramatically from octahedral to tetrahedral (see Figures 3 and 4). The 50-15-35 glass has nearly 75% of the aluminum in Al(4) environments and only 9% in Al(6) environments. The amount of five-coordinated aluminum, Al(5), also increases as αAl_2O_3 is added, but levels off at approximately 20% at $x \geq 10$ mole% αAl_2O_3.

$^{31}P/^{27}Al$ Dipolar Dephasing NMR. The $^{31}P/^{27}Al$ dipolar dephasing NMR spectra of the 50-2.5-47.5 NAP glass are shown on the left-hand side of Figure 5. The ^{31}P reference spectrum, which is analogous to a Hahn echo experiment with $\tau = 5$ ms, is shown at top. The middle spectrum displays the results of the experiment with ~50 kHz irradiation applied to the ^{27}Al nuclei throughout the dephasing time (τ). Subtraction of the middle spectrum from the reference spectrum yields the so-called dipolar dephasing difference, or TRAPDOR difference (ΔS) spectrum shown at bottom. Clearly the aluminum incorporated to form the 50-2.5-47.5 glass shows preferential coordination to the new ^{31}P resonance at $\delta = -7.1$ ppm. This can be assigned to either a $Q^1(1Al)$ or $Q^1(2Al)$ phosphorus environment.[9,12,57,58] The effects of the dipolar dephasing experiment also impacts the $Q^2(0Al)$ or upfield phosphorus, but has no effect on the $Q^1(0Al)$ phosphorus. This is supported by the ^{31}P MAS NMR results as well, which show the chemical shift of the $Q^2(0Al)$ species changing as the mole% alumina increases, while the chemical shift of the $Q^1(0Al)$ specie stays relatively constant (see Table 1). The $^{31}P/^{27}Al$ dipolar

dephasing experiment of the 50-10-40 glass is shown in the middle column of Figure 5, the arrangement of the spectra being analogous to those of the 50-2.5-47.5 glass. Once again, the aluminum species in this glass shows strong dipolar coupling with the $Q^1(m\text{Al})$ species but no coupling with the $Q^1(0\text{Al})$ species. Finally, the $^{31}P/^{27}Al$ dipolar dephasing NMR experiment for the 50-15-35 glass is shown in Figure 5 to the right. No longer are the effects of irradiating the ^{27}Al nuclei during the dephasing time τ specific to a few phosphorus environments; rather, all the phosphorus environments in this glass are affected, with a slight preference to the upfield resonances.

$^{31}P/^{23}Na$ Dipolar Dephasing NMR. Results of the dipolar dephasing experiments with $\tau = 3$ ms for the 50-2.5-47.5, 50-10-40, and 50-15-35 glasses are shown in Figure 6. In these experiments, all of the ^{31}P environments are affected by the ^{23}Na irradiation. As the mole% sodium is constant (50%) throughout this entire glass series, few, if any, structural bonding scenarios of phosphorus without coordination to sodium are expected. In the 50-2.5-47.5 glass (shown to the left in Figure 6), the $Q^1(m\text{Al})$ phosphorus (–7.1 ppm) and the $Q^1(0\text{Al})$ phosphorus (+1.7 ppm) environments are proportionately reduced in the dipolar dephasing experiment while the $Q^2(0\text{Al})$ phosphorus specie (–18.7 ppm) displays a less pronounced effect. This implies that the dipolar coupling between ^{23}Na and ^{31}P is greater for the $Q^1(m\text{Al})$ and $Q^1(0\text{Al})$ environments than in the $Q^2(0\text{Al})$ environments, i.e., that the ^{23}Na to ^{31}P bond distance is shorter or that the number of ^{23}Na affecting the ^{31}P environment is greater. For the 50-10-40 and 50-15-35 glasses all of the phosphorus environments appear proportionally affected.

$^{31}P/^{23}Na$ dipolar dephasing NMR experiments with irradiation times ranging from 0.4 to 10 ms were performed on all of the NAP glasses studied and are shown in Figure 7. In

addition, to address the possible impact of ionic motion, and perhaps better resolve the various ^{31}P environments dipolar coupled to ^{23}Na, $^{31}P/^{23}Na$ dipolar dephasing experiments were also performed at a lower temperature, 200K. The difference spectra, ΔS, generated at 200K, however, are indistinguishable versus those at ambient temperature, which implies that ionic motion has minimal impact at 200K. Our results are presented here using the experiments performed at ambient temperature.

Discussion

Utilizing these NMR results, a better understanding regarding the MRO and structural evolution occurring in the near-metaphosphate base glass as a function of aluminum incorporation can be detailed. The structure of the sodium metaphosphate glass (50-0-50) consist of chains of $Q^2(0Al)$ phosphate tetrahedra having moderate length terminated by $Q^1(0Al)$ end species.[6,8,19] While the RFDR experiment performed on this sample does not definitively rule out the concomitant existence of $Q^2(0Al)$ phosphate ring structures and $Q^1(0Al)$ diphosphate regions, it does clearly define the $Q^2(0Al)$ and $Q^1(0Al)$ chain motif as the preferred structure.

Incorporating aluminum into the sodium near-metaphosphate glass results in depolymerization of the $Q^2(0Al)$ chain structure. The predicted pathways for aluminum integration are primarily two-fold: (1) either the aluminum replaces a sodium atom on one of the non-bridging oxygens (NBO) associated with a $Q^2(0Al)$ or $Q^1(0Al)$ tetrahedra; or (2) the aluminum incorporates into the glass structure by breaking a P-O-P bond and forming a bridging P-O-Al bond, with the $Q^2(0Al)$ tetrahedral species becoming a $Q^1(1Al)$ tetrahedra. Aluminum integration via the first pathway is expected to increase

the shielding on the phosphorus nucleus thereby making the ^{31}P chemical shift more negative.[58] This trend is not observed in the ^{31}P NMR spectra following the addition of alumina (see Figure 2). Formation of P-O-Al bonds via the second pathway is predicted to decrease the shielding on the phosphorus nucleus thereby making the chemical shift more positive. The 1D ^{31}P, and the $^{31}P/^{27}Al$ and $^{31}P/^{23}Na$ dipolar dephasing NMR results support this as the dominant depolymerization pathway. In the 50-0-50 base glass 90% of the phosphorus tetrahedra reside in a $Q^2(0Al)$ environment (see Table 1). After addition of 2.5 mole% alumina the percentage of $Q^2(0Al)$ sites is reduced to 69%, the amount of $Q^1(mAl)$ environments created are 21%, and the percentage of phosphorus in $Q^1(0Al)$ tetrahedra remains unchanged at 10%. The conversion of $Q^2(0Al)$ to $Q^1(mAl)$ appears to be the dominant structural rearrangement pathway for glass compositions through 50-7.5-42.5, (i.e., $P_{Q^2(0Al)} + P_{Q^1(mAl)} = 90\%$, see Table 1). In fact, $P_{Q^2(0Al)} + P_{Q^1(mAl)} \cong 90\%$ through the 50-12.5-37.5 composition, implying that the depolymerization process involves primarily the formation of $Q^1(mAl)$ species between 7.5 and 12.5 mole% alumina, and that the $Q^1(0Al)$ species are not largely affected by the addition of Al ($P_{Q^1(0Al)} \approx 10\%$). This conclusion is supported by the ^{31}P NMR resonances between 0 and –14 ppm that continue to show dipolar coupling to aluminum in the $^{31}P/^{27}Al$ dipolar dephasing experiments, while the $Q^1(0Al)$ sites are nullified in the ΔS spectra (see Figure 5).

The assignment of these new ^{31}P NMR resonances has remained controversial.[9,41,57-59]. Dollase et al. investigation of orientationally disordered crystals (ODC) in the series $Na_{3-3x}Al_xPO_4$ reported that a ^{31}P NMR resonance between –3.5 ppm and –5 ppm is assigned to a $Q^1(2Al)$ phosphate tetrahedral species.[58] Brow et al. thus suggested that the

resonance forming between –8 and –11 ppm in an analogous amorphous aluminophosphate system might be attributed to $Q^1(2Al)$ environments.[57] One scenario they proposed was that two $-O^-Na^+$ species are replaced by two –OAl(6) species on a $Q^1(0Al)$ tetrahedron thereby causing the displacement of the chemical shift to more negative values relative to the ~ +2 ppm for $P(OP)(O^-Na^+)_3$. The $^{31}P/^{27}Al$ and $^{31}P/^{23}Na$ dipolar dephasing results presented in this manuscript, however, show that the initial aluminum incorporates not by replacing $-O^-Na^+$ bonds, but, rather, by replacing P-O-P bonds with P-O-Al bonds. To the best of our knowledge, this is the first experiment showing decisively that the added aluminum incorporates preferentially within the $Q^2(0Al)$ chain rather than to terminal $Q^1(0Al)$ species. As it seems unlikely that the dominant depolymerization pathway would be directly from $Q^2(0Al)$ to $Q^1(2Al)$ at only 2.5 mole% alumina, we attribute the new phosphorus resonance at –7.1 ppm to the formation of $Q^1(1Al)$ species. These species show strong dipolar coupling with the added aluminum, and the upfield tailing of this resonance implies that either a small amount of another $Q^1(mAl)$ species exists, or that the $Q^2(0Al)$ specie is also dipolar coupled to the aluminum (see Figure 5). Interestingly, the $Q^1(0Al)$ species are completely eliminated in the difference spectrum of the 50-2.5-47.5 glass, implying that they have no dipolar coupling with the added aluminum. The lack of $Q^0(mAl)$ formation at low Al concentrations also demonstrates that cleavage of the $Q^1(0Al)$ end groups does not occur.

The 50-2.5-47.5 glass has an O/P ratio close to 3.1, and its ^{27}Al MAS NMR spectrum shows 86% of the aluminum as having octahedral coordination (see Table 2). Thus, the proposal of the ^{31}P resonance at –7.1 ppm to a $Q^1(1Al)$ environment leaves a local charge balancing question. Namely, if the attached aluminum in an $Q^1(1Al)$ environment is

Al(6) then one of the terminal oxygens will be underbonded and require coordinating to multiple sodium ions in order to obtain charge neutrality. Even though a significant fraction of Al(5) and Al(4) are present in all compositions to assist in charge balancing, previous work on similar glass systems have often submitted that the resonance between –6 and –11 ppm is due to $Q^1(2Al)$ species, which are charge neutral when all of the NNN aluminum nuclei are Al(6).[9,41,57] Recent work by Belkébir et al., however, proposes that a disproportionation of diphosphate species into triphosphate and monophosphate ions crosslinked by aluminum atoms whose average coordination increases accounts for the ^{31}P resonance near –7 ppm.[59] As their solution ^{31}P NMR results reveal a large proportion of diphosphate still present in the glass with O/P ratio 3.5 (50-10-40), it did not seem reasonable to assign the resonance at ~ –7 ppm to $Q^0(mAl)$ or $Q^2(0Al)$ species. Thus, in the deconvolution of their solid-state ^{31}P NMR spectra they propose that the resonances at –6.8 ppm and ~ –16 ppm belong to $P(OP)(OAl)(ONa_y)_2$, $Q^1(1Al)$, and $P(OP)(OAl)_2(ONa_y)$ species, $Q^1(2Al)$, respectively. Here the value of '*y*' is not obvious to specify as the coordination of the oxygen does not remain equal to two.[59] The presence of multiple cationic environments, in conjunction with the existence of Al(4) and Al(5) environments, helps address the charge balancing question and give credibility to assigning the ^{31}P resonance at –7.1 ppm to a $Q^1(1Al)$ specie.

With the addition of 10 mole% alumina, the $Q^1(1Al)$ environment dominates the phosphorus spectrum and the preferred coordination of aluminum is changing from Al(6) to Al(4), with ~20% remaining as Al(5). This change in coordination coincides with the increase in the O/P ratio of the glass. When O/P = 3.0 (50-0-50 glass) the preferred phosphate structure is the metaphosphate Q^2 chain. When O/P = 3.5 (50-10-40) the

preferred structure is expected to be pyrophosphate.[5] While a crystalline $Q^1(3Al)$ structure can support three Al(6) environments and remain charge balanced,[54] if the O/P ratio becomes > 3.5, the aluminum must take on a lower coordination state to keep the system charge neutral.[9] Deconvolution of the 50-10-40 ^{31}P MAS spectrum yields chemical shift values of –12.0, –5.4 and +1.6 ppm (see Table 1). The change in the chemical shift values for the $Q^1(2Al)$ and $Q^1(1Al)$ species are +1.6 and +1.7 ppm, respectively, versus the 50-2.5-47.5 glass, while the change to the $Q^1(0Al)$ specie is negligible. The $^{31}P/^{27}Al$ dipolar dephasing experiment, Figure 5, singles out only the –12.0 and –5.4 ppm environments as being dipolar coupled to aluminum. Once again, the $Q^1(0Al)$ specie is absent from the difference spectrum, ΔS. Knowing that additional NNN aluminum atoms will make a $Q^1(1Al)$ phosphorus more negative,[58] one plausible depolymerization scenario occurring at the pyrophosphate transition point (O/P=3.5) is that a portion of the $Q^1(1Al)$ species are modified to $Q^1(2Al)$ species while the remaining $Q^2(0Al)$ species are depolymerized to $Q^1(1Al)$ species. Both Belkébir et al.[59] and Egan et al.[41] also note the existence of $Q^1(2Al)$ species for O/P ratio ~ 3.5. Egan et al., however, who acquired some of their data using cross-polarization from ^{27}Al to ^{31}P, attribute the ^{31}P NMR resonance they see at ~ –11 ppm to a $Q^0(3Al)$ species and the resonance at ~ –6 ppm to a $Q^1(2Al)$ species. A $Q^0(3Al)$ species is made charge neutral with one Al(6) and two Al(4) NNN, while a $Q^1(2Al)$ species is made charge neutral with two Al(6) NNN.[9] In the 2D CPMAS correlation spectrum of Egan et al.[41] both sites show coordination to the Al(4) and Al(6) aluminum nuclei, but only the $Q^1(2Al)$ species shows coordination to Al(5) aluminum. Being able to assign a phosphorus resonance to a specific coordinated aluminum nuclei is a very nice feature of this technique. As stated above though, we

assign the ^{31}P resonance at –12 ppm in our spectrum to a $Q^1(2Al)$ species. At or below an O/P ratio of 3.5, the depolymerization of phosphorus into an alumino-orthophosphate species, e.g., $Q^0(3Al)$, does not appear to be a prominent reaction. Actually, the ODC investigation done by Dollase et al. found phosphorus nuclei in $Q^0(3Al)$ environments to be more shielded and to resonate at ~ –15 ppm.[58]

At 15 mole% alumina the depolymerization of Q^2 tetrahedra appears complete. We attribute the phosphorus resonances observed at –9.5 ppm (24%), -2.7 ppm (62%) and +6.3 ppm (14%) to $Q^1(2Al)$, $Q^0(2Al)$[58] and $Q^0(1Al)$[58] environments, respectively. As all these environments have aluminum as NNN, the $^{31}P/^{27}Al$ dephasing difference spectrum displays the expected dipolar coupling between ^{27}Al and ^{31}P in all of them (see Figure 5). Interestingly, our $^{31}P/^{27}Al$ dipolar dephasing results have shown throughout that all of the new ^{31}P resonances formed during the incorporation of alumina are dipolar coupled to aluminum.

Figure 6 shows the $^{31}P/^{23}Na$ dipolar dephasing results of the same NAP glasses displayed in Figure 5. As the mole% sodium remains fixed at 50 throughout our entire glass series, it is not too surprising that all of the phosphorus environments show dipolar coupling to sodium. More importantly though, the dipolar dephasing difference as a function of decoupling pulse duration (see Figure 7) clearly shows that the ^{23}Na-^{31}P dipolar coupling environment is not changed with increasing alumina incorporation. This supports our conclusions based on the previously discussed $^{31}P/^{27}Al$ dipolar dephasing results that at lower αAl_2O_3 concentrations the aluminum incorporates by replacing P-O-P bonds with P-O-Al bonds not by replacing $-O^-Na^+$ bonds. This invariant sodium-phosphorus environment implies that large structural changes in the Na-P bonding does

not occur for this glass series, and that any observed changes in the physical properties of the glass must be a result of changes in the Al-P and P-O bonding environments.

Conclusions

Based on the multi-nuclear NMR experimental results, we propose a depolymerization and structural modification pathway for the $xAl_2O_3 \cdot 50Na_2O \cdot (50\text{-}x)P_2O_5$ ($0 \leq x \leq 17.5$) glass system studied using $Q^2(0Al) \rightarrow Q^1(1Al) \rightarrow Q^1(2Al) \rightarrow Q^0(2Al)$ and $Q^1(0Al) \rightarrow Q^0(1Al)$ reaction sequences. When the mole% alumina is lower than 10 (O/P ratio < 3.5) the preferred structure of the glass are modified metaphosphate $Q^2(0Al)$ chains.[5] Adding alumina depolymerizes the glass structure by breaking P-O-P bonds and forming P-O-Al bonds, e.g., $Q^2(0Al) \rightarrow Q^1(1Al)$. The $Q^1(0Al)$ environments are not affected by the added alumina until after the O/P ratio is greater than 3.5.

For O/P ratios greater than 3.5 (mole% Al > 10) the preferred coordination of aluminum is tetrahedral, Al(4). Concomitantly, no longer does the phosphorus reside in a $Q^2(0Al)$ structure. Rather, all of the $Q^2(0Al)$ sites have been converted into $Q^1(1Al)$ species, which are then further depolymerized into $Q^1(2Al)$ species. Beyond 10 mole% alumina, the depolymerization of the Q^2 chain appears complete, with $Q^0(2Al)$ being the dominant phosphorus environment. Finally, when the mole% alumina is greater than 12.5, depolymerization occurs to the $Q^1(0Al)$ tetrahedral species as well, with $Q^1(0Al)$ becoming $Q^0(1Al)$.

The NMR results demonstrate that by combining $^{31}P/^{27}Al$ and $^{31}P/^{23}Na$ dipolar dephasing experiments with classical 1D ^{31}P and ^{27}Al MAS NMR experiments, detailed structural information about a glass system can be obtained, including the relative

distribution of modifying cations with respect to the phosphate backbone. Such structural information also provides insight for analyzing many of the glass dissolution mechanisms that are presently being investigated in our laboratory.

Acknowledgements

The authors would like to express their thanks and appreciation to Dr. Richard Brow for his careful reading and suggestions for making this manuscript more complete. Sandia is a multiprogram laboratory operated by Sandia Corporation, a Lockheed Martin Company for the United States Department of Energy under Contract DE-AC04-94AL85000.

References

(1) Wilder, J. A. *J. Non-Cryst. Solids* **1980**, *38&39*, 879.

(2) Brow, R. K.; Kovacic, L.; Loehman, R. E. *Ceram. Trans.* **1996**, *70*, 177.

(3) Weber, M. J. *J. Non-Cryst. Solids* **1990**, *123*, 208.

(4) Payne, S. A.; Elder, M. L.; Campbell, J. H.; Wilke, G. D.; Weber, M. J.; Hayden, Y. T. *Solid State Optical Materials* **1992**, *28*, 253.

(5) Brow, R. K. *J. Am. Ceram. Soc.* **1993**, *76*, 913.

(6) van Wazer, J. R. *Phosphorus and Its Compounds*; Interscience: New York, 1958; Vol. 1.

(7) Feike, M.; Graf, R.; Schell, I.; Jager, C.; Speiss, H. W. *J. Am. Chem. Soc.* **1996**, *118*, 9631.

(8) Martin, S. W. *Eur. J. Solid State Inorg. Chem.* **1991**, *28*, 163.

(9) Brow, R. K.; Kirkpatrick, R. J.; Turner, G. L. *J. Am. Ceram. Soc.* **1993**, *76*, 919.

(10) Kreidl, N. J.; Weyl, W. A. *J. Am. Ceram. Soc.* **1941**, *24*, 372.

(11) Eckert, H. *Progress in NMR Spectroscopy* **1992**, *24*, 159.

(12) Kirkpatrick, R. J.; Brow, R. K. *Solid State Nuclear Magnetic Resonance* **1995**, *5*, 9.

(13) Brow, R. K. *J. Non-Cryst. Solids* **2000**, *263&264*, 1.

(14) Jäger, C.; Feike, M.; Born, R.; Spiess, H. W. *J. Non-Cryst. Solids* **1994**, *180*, 91.

(15) Born, R.; Feike, M.; Jäger, C.; Spiess, H. W. *Z. Naturforsch.* **1995**, *50*, 169.

(16) Alam, T. M.; Brow, R. K. *J. Non-Cryst. Solids* **1998**, *223*, 1.

(17) Hartmann, P.; Vogel, J.; Friedrich, U.; Jäger, C. *J. Non-Cryst. Solids* **2000**, *263&264*, 94.

(18) Feike, M.; Demco, D. E.; Graf, R.; Gotwald, J.; Hafner, S.; Speiss, H. W. *J. Magn. Reson. A* **1996**, *122*, 214.

(19) Feike, M.; Jager, C.; Spiess, H. W. *J. Non-Cryst. Solids* **1998**, *223*, 200.

(20) Hartmann, P.; Jana, C.; Vogel, J.; Jäger, C. *Chem. Phys. Lett.* **1996**, *258*, 107.

(21) Lee, Y. K.; Kurur, N. D.; Helmle, M.; Johannessen, O. G.; Nielsen, N. C.; Levitt, M. H. *Chem. Phys. Lett.* **1995**, *242*, 304.

(22) Blackwill, C. S.; Patton, R. L. *J. Phys. Chem.* **1984**, *88*, 6135.

(23) Vega, A. J. *J. Magn. Res.* **1992**, *96*, 50.

(24) Vega, A. J. *Solid State NMR* **1992**, *1*, 17.

(25) Guillon, T.; Schaefer, J. *J. Magn. Reson.* **1989**, *81*, 196.

(26) Pan, Y.; Guillon, T.; Schaefer, J. *J. Magn. Res.* **1990**, *90*, 330.

(27) Fyfe, C. A.; Mueller, K. T.; Grondey, H.; Wong-Moon, K. C. *Chem. Phys. Lett.* **1992**, *199*, 198.

(28) Hing, A. W.; Vega, S.; Schaefer, J. *J. Magn. Res.* **1992**, *96*, 205.

(29) van Eck, E. R. H.; Janssen, R.; Maas, W. E. J. R.; Veeman, W. S. *Chem. Phys. Lett.* **1990**, *175*, 428.

(30) Grey, C. P.; Veeman, W. S.; Vega, A. J. *J. Chem. Phys.* **1993**, *98*, 7711.

(31) Grey, C. P.; Vega, A. J. *J. Am. Chem. Soc.* **1995**, *117*, 8232.

(32) Fyfe, C. A.; Wong-Moon, K. C.; Huang, Y.; Grondey, H.; Mueller, K. T. *J. Phys. Chem.* **1995**, *99*, 8707.

(33) Guillon, T. *J. Magn. Reson. A* **1995**, *117*, 8232.

(34) Sachleben, J. R.; Frydman, V.; Frydman, L. *J. Am. Chem. Soc.* **1996**, *118*, 9786.

(35) Herzog, K.; Thomas, B.; Sprenger, D.; Jäger, C. *J. Non-Cryst. Solids* **1995**, *190*, 296.

(36) van Wüllen, L.; Züchner, L.; Müller-Warmuth, W.; Eckert, H. *Solid State NMR* **1996**, *6*, 203.

(37) Schaller, T.; Rong, C.; Toplis, M. J.; Cho, H. *J. Non-Cryst. Solids* **1999**, *248*, 19.

(38) Wenslow, R. M.; Mueller, K. T. *J. Non-Cryst. Solids* **1998**, *231*, 78.

(39) Wenslow, R. M.; Mueller, K. T. *J. Phys. Chem. B* **1998**, *102*, 9033.

(40) Zeng, Q.; Nekvasil, H.; Grey, C. *J. Phys. Chem. B* **1999**, *103*, 7406.

(41) Egan, J. M.; Wenslow, R. M.; Mueller, K. T. *J. Non-Cryst. Solids* **2000**, *261*, 115.

(42) Prabakar, S.; Wenslow, R. M.; Mueller, K. T. *J. Non-Cryst. Solids* **2000**, *263&264*, 82.

(43) van Eck, E. R. H.; Veeman, W. S. *J. Am. Chem. Soc.* **1993**, *115*, 1168.

(44) Kao, H.-M.; Grey, C. *J. Phys. Chem.* **1996**, *100*, 5106.

(45) Rocha, J.; Lourence, J. P.; Ribeiro, M. F.; Fernandez, C.; Amoureux, J. P. *Zeolites* **1997**, *2/3*, 156.

(46) Fernandez, C.; Amoureux, J. P.; Chezeau, J. M.; Delmotte, L.; Kessler, H. *Microporous Mater.* **1996**, *6*, 331.

(47) Fernandez, C.; Delevoye, L.; Amoureux, J. P.; Lang, D. P.; Pruski, M. *J. Am. Chem. Soc.* **1997**, *119*, 6858.

(48) Pruski, M.; Lang, D. P.; Fernandez, C.; Amoureux, J. P. *Solid State NMR* **1997**, *7*, 327.

(49) Pruski, M.; Bailly, A.; Lang, D. P.; Amoureux, J. P.; Fernandez, C. *Chem. Phys. Lett.* **1999**, *307*, 35.

(50) Fernandez, C.; Lang, D. P.; Amoureux, J. P.; Pruski, M. *J. Am. Chem. Soc.* **1998**, *120*, 2672.

(51) Taulelle, F.; Pruski, M.; Amoureux, J. P.; Lang, D. P.; Bailly, A.; Huguenard, C.; Haouas, M.; Gérardin, C.; Loiseau, T.; Férey, G. *J. Am. Chem. Soc.* **1999**, *121*, 12148.

(52) vander Meer, H. *Acta Crystallogr. Sect. B* **1976**, *32*, 2423.

(53) Thong, N.; Schwarzenbach, D. *Acta Crystallogr. Sect. A* **1979**, *35*, 658.

(54) Ng, H. N.; Calvo, C. *Can. J. Chem.* **1973**, *51*, 2613.

(55) Herzfeld, J.; Berger, A. E. *J. Chem. Phys.* **1980**, *73*, 6021.

(56) Brow, R. K.; Phifer, C. C.; Turner, G. L.; Kirkpatrick, R. J. *J. Am. Ceram. Soc.* **1991**, *74*, 1287.

(57) Brow, R. K.; Kirpatrick, R. J.; Turner, G. L. *J. Non-Cryst. Solids* **1990**, *116*, 39.

(58) Dollase, W. A.; Merwin, L. H.; Sebald, A. *J. Solid State Chem* **1989**, *83*, 140.

(59) Belkébir, A.; Rocha, J.; Esculcas, A. P.; Berthet, P.; Gilbert, B.; Gabelica, Z.; Llabres, G.; Wijzen, F.; Rulmont, A. *Spectrochimica Acta A* **1999**, *55*, 1323.

Figure Captions

Figure1. The dipolar dephasing pulse sequence is applied under MAS conditions with rotational period, τ_r. It consists of two parts: (a) a spin echo acquired without S spin decoupling (due to high attenuation on the S channel amplifier), and (b) repeating the spin echo experiment with application of a 50 kHz rf decoupling pulse to the S nuclei.

Figure 2. ^{31}P MAS NMR spectra of NAP glasses with molar percent composition $50Na_2O{\cdot}xAl_2O_3{\cdot}(50\text{-}x)P_2O_5$.

Figure 3. ^{27}Al MAS NMR spectra of NAP glasses with molar percent composition $50Na_2O{\cdot}xAl_2O_3{\cdot}(50\text{-}x)P_2O_5$.

Figure 4. Percent of aluminum existing in each coordination state (RA) as a function of the mole% aluminum in the NAP glass series.

Figure 5. ^{31}P/^{27}Al dipolar dephasing results of the 50-2.5-47.5 (left), 50-10-40 (middle) and 50-15-35 (right) NAP glasses. The top spectra are acquired without irradiation of the ^{27}Al nuclei. The spectra in the center were acquired with 50kHz irradiation applied to the ^{27}Al nuclei. The bottom spectra show the dipolar dephasing difference for τ = 5 ms, ΔS, resulting from each experiment.

Figure Captions

Figure 6. $^{31}P/^{23}Na$ dipolar dephasing results of the 50-2.5-47.5 (left), 50-10-40 (middle) and 50-15-35 (right) NAP glasses. The top spectra are acquired without irradiation of the ^{23}Na nuclei. The spectra in the center were acquired with 50kHz irradiation applied to the ^{23}Na nuclei. The bottom spectra show the dipolar dephasing difference $\tau = 5ms$, ΔS, resulting from each experiment.

Figure 7. The $^{31}P/^{23}Na$ dipolar dephasing difference amplitudes versus decoupling pulse duration,τ. The relatively constant slope for the entire NAP glass series implies that the addition of ^{27}Al does not result in the extensive replacement of ^{23}Na by ^{27}Al, but, rather, by the replacement of P-O-P bounds with P-O-Al bounds.

Table Captions

Table 1. ^{31}P isotropic chemical shift assignments, relative populations, and T_g data for the NAP glass series. [a] Batch composition: e.g., a glass labeled 50-10-40 is batched (in mole%) as $50Na_2O \cdot 10Al_2O_3 \cdot 40P_2O_5$. [b] Bond types: e.g., notation $Q^2(0Al)$ denotes that each P has two bridging bonds to other phosphorus nuclei and zero bridging bonds to aluminum nuclei. [c] Isotropic chemical shift referenced to a secondary external reference $(NH_4)H_2PO_4$ (δ = 0.8 ppm with respect to phosphoric acid, δ = 0.0 ppm). [d] Fractional population, obtained from simulation of the entire MAS NMR sideband manifold. [e] Onset of glass transition temperature measured by DSC. [f] Onset of crystallization measured by DSC.

Table 2. Relative peak area (RA) and chemical shift values for Al(4), Al(5) and Al(6) coordinated aluminum as a function of mole percent aluminum.

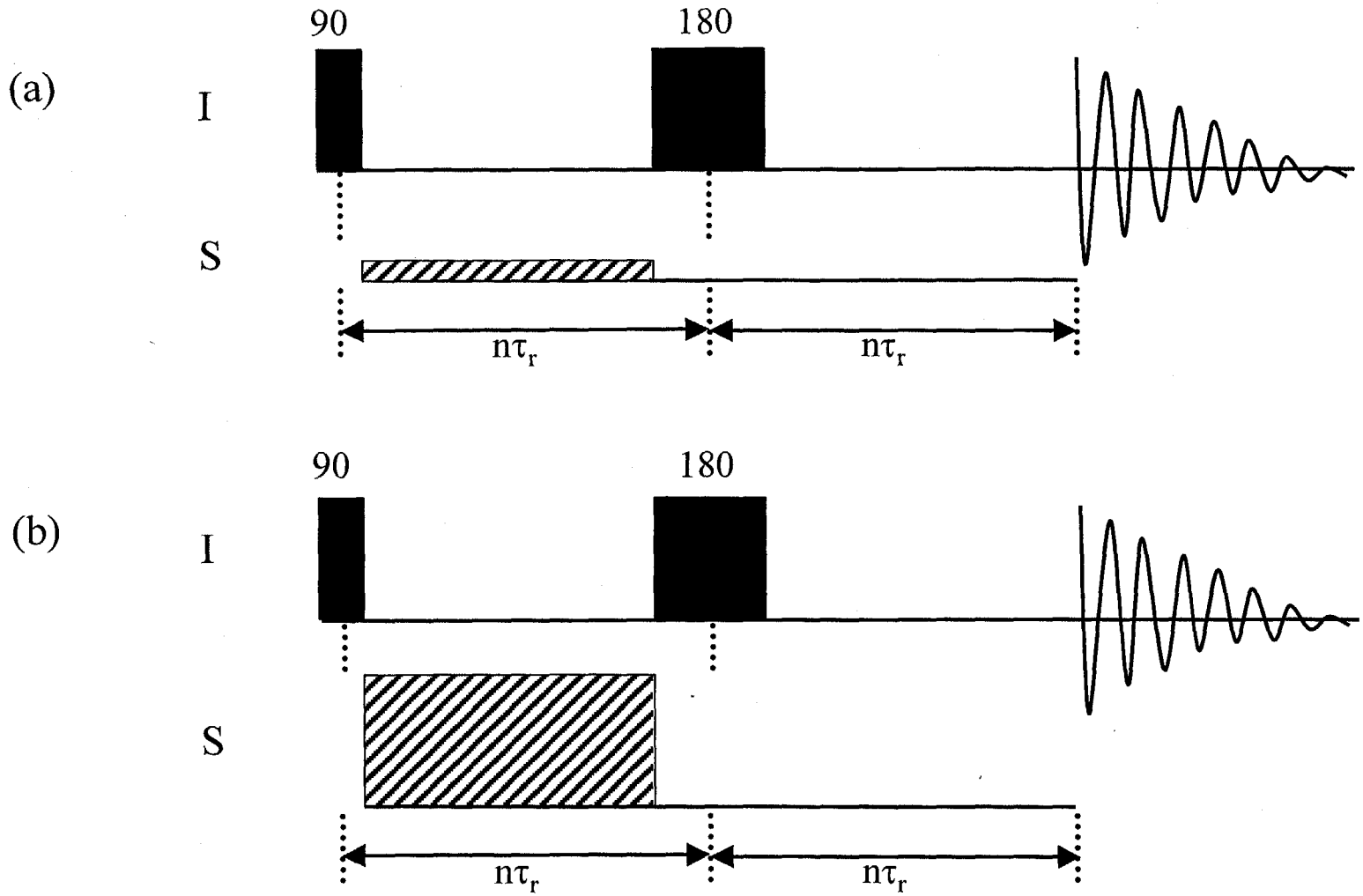

Figure 1. Lang et al.

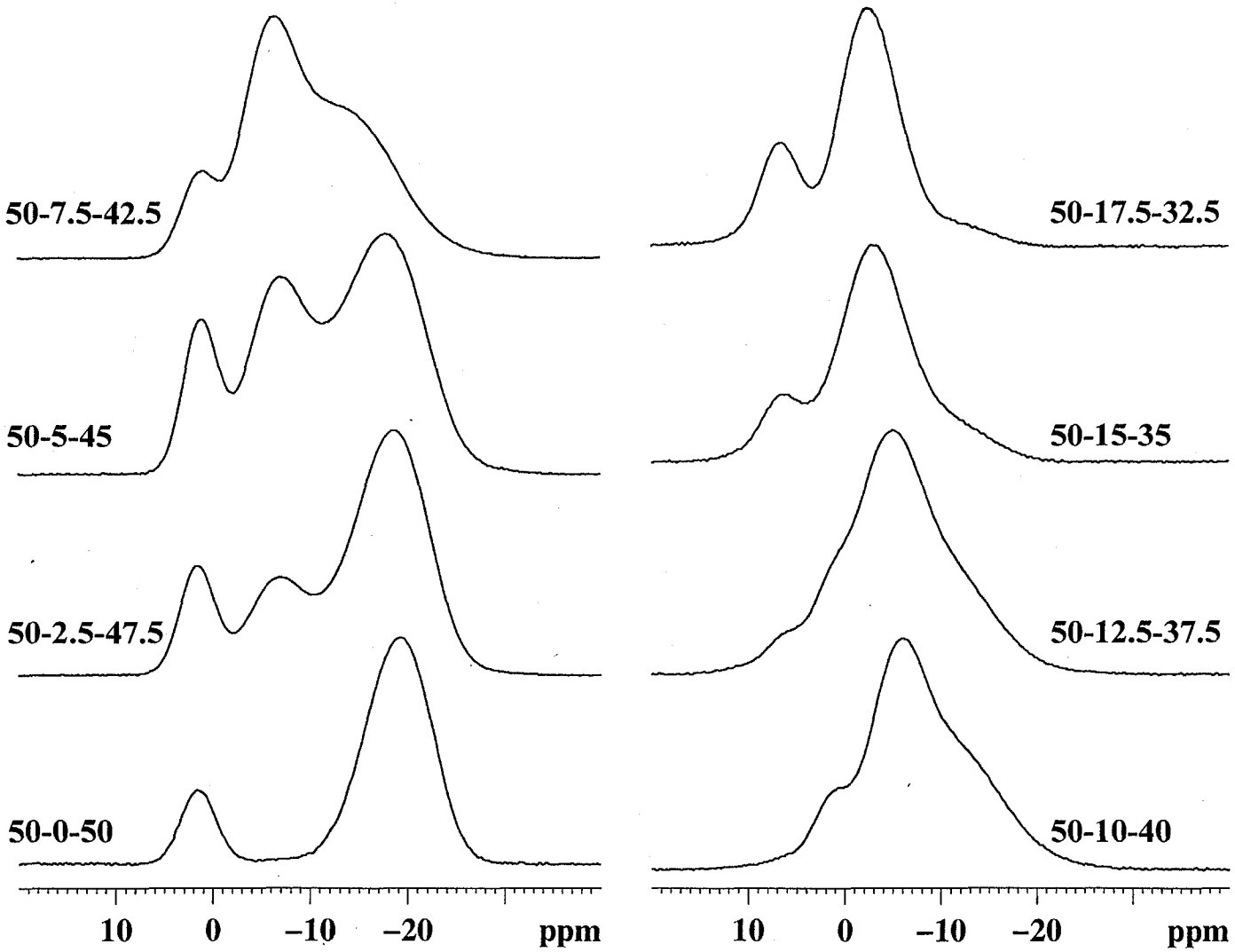

Figure 2. Lang et al.

NAP Glass Composition[a]	Bond Type[b]	δ_{iso} (ppm)[c]	P_{Q^n} [d]	T_g[e](°C)	T_x[f](°C)
50-0-50	$Q^2(0Al)$	-19.3	0.90	287	343
	$Q^1(0Al)$	+ 1.5	0.10		
50-2.5-47.5	$Q^2(0Al)$	-18.7	0.69	301	406
	$Q^1(0Al)$	+ 1.6	0.10		
	$Q^1(1Al)$	- 7.1	0.19		
	$Q^1(2Al)$	-13.6	0.02		
50-5-45	$Q^2(0Al)$	-18.9	0.57	323	431
	$Q^1(0Al)$	+ 1.2	0.11		
	$Q^1(1Al)$	- 6.4	0.24		
	$Q^1(2Al)$	-13.6	0.08		
50-7.5-42.5	$Q^2(0Al)$	-18.8	0.10	390	479
	$Q^1(0Al)$	+ 1.3	0.09		
	$Q^1(1Al)$	- 5.9	0.44		
	$Q^1(2Al)$	-13.6	0.37		
50-10-40	$Q^1(0Al)$	+ 1.6	0.10	393	447
	$Q^1(1Al)$	- 5.4	0.48		
	$Q^1(2Al)$	-12.0	0.42		
50-12.5-37.5	$Q^1(0Al)$	+ 1.6	0.09	368	425
	$Q^1(1Al)$	- 5.5	0.16		
	$Q^1(2Al)$	- 9.6	0.44		
	$Q^0(1Al)$	+ 6.3	0.06		
	$Q^0(2Al)$	- 2.7	0.25		
50-15-35	$Q^1(2Al)$	- 9.5	0.24	350	415
	$Q^0(1Al)$	+ 6.3	0.14		
	$Q^0(2Al)$	- 2.7	0.62		
50-17.5-32.5	$Q^1(2Al)$	- 9.3	0.11	358	405
	$Q^0(1Al)$	+ 6.7	0.20		
	$Q^0(2Al)$	- 2.5	0.69		

Table 1. Lang et al.

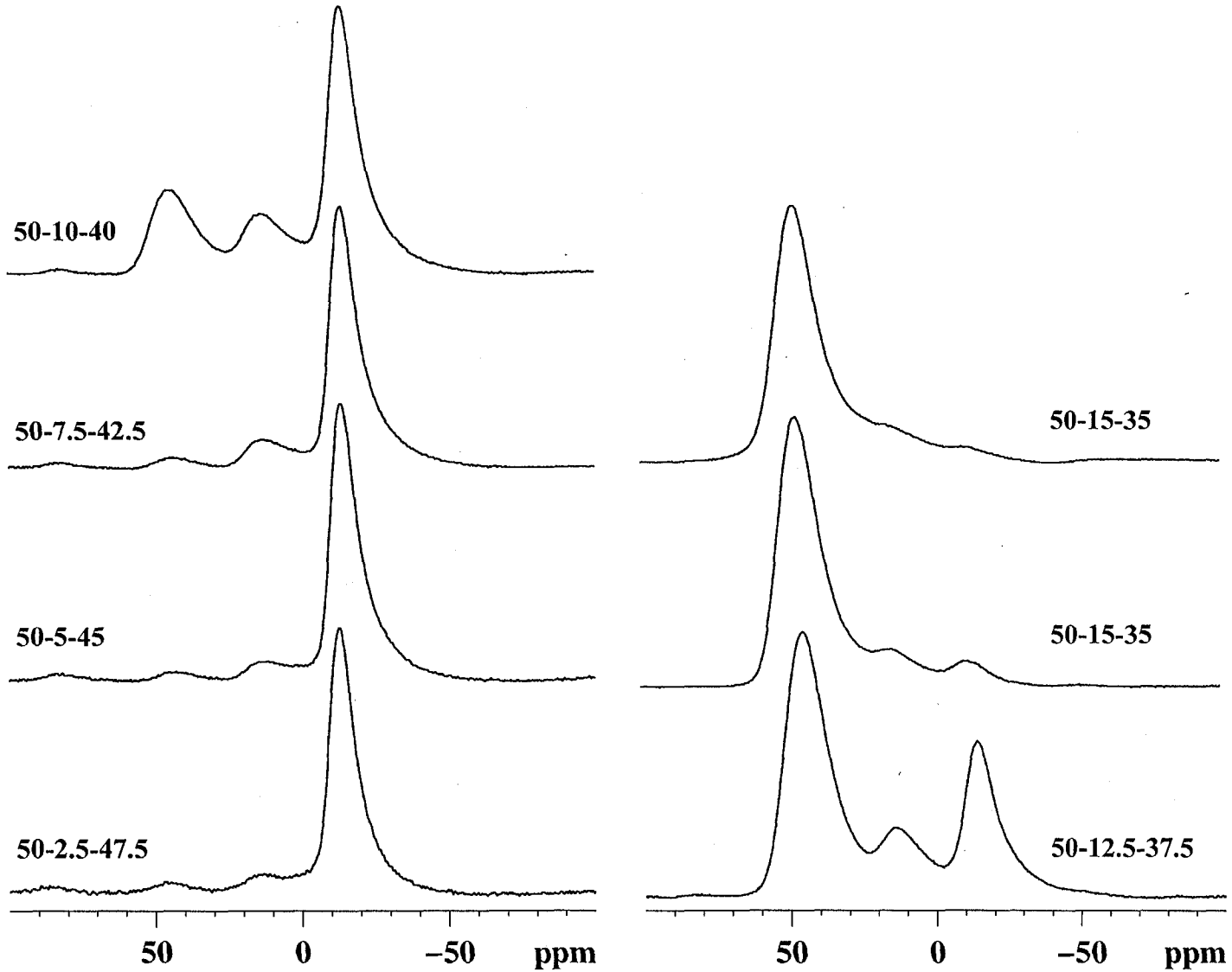

Figure 3. Lang et al.

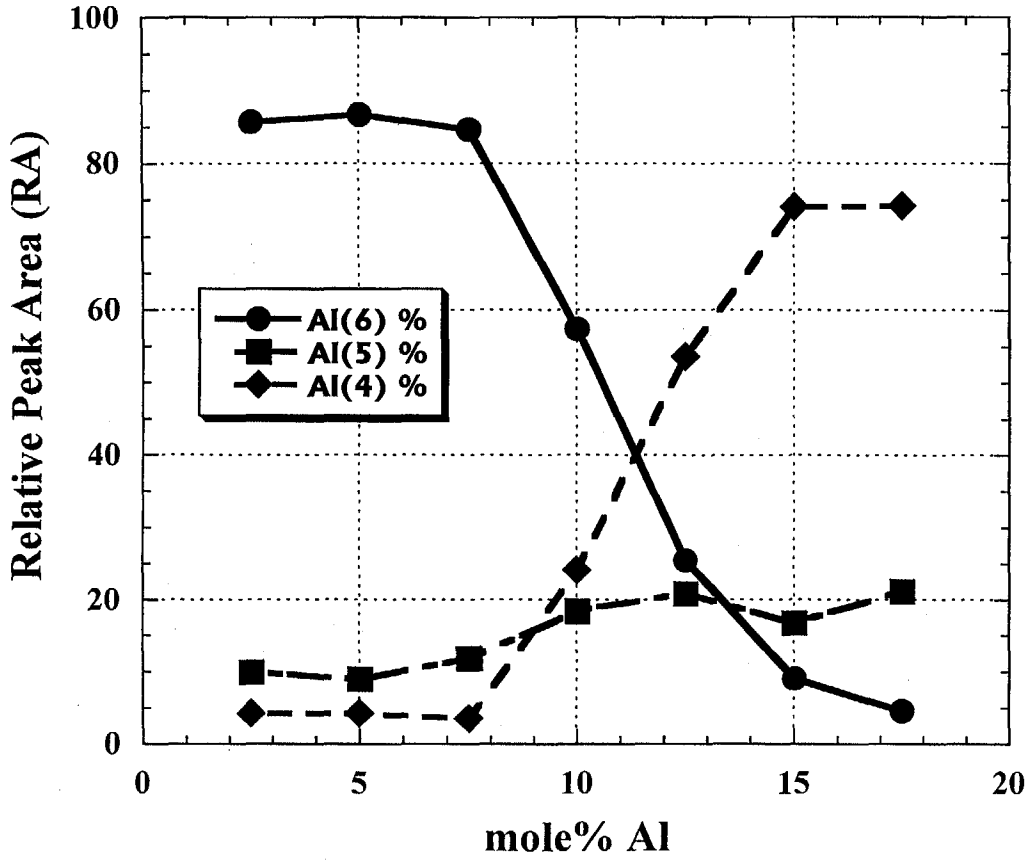

Figure 4. Lang et al.

NAP Glass Composition	Al(6) δ_{ppm}	Al(5) δ_{ppm}	Al(4) δ_{ppm}
50-2.5-47.5	-13.7	11.4	44.6
50-5-45	-13.0	11.5	42.9
50-7.5-42.5	-14.7	11.7	43.0
50-10-40	-14.6	12.8	43.4
50-12.5-37.5	-13.7	14.0	45.0
50-15-35	-12.1	14.8	46.0
50-17.5-32.5	-12.3	18.0	46.0

NAP Glass Composition	Al(6) RA	Al(5) RA	Al(4) RA
50-2.5-47.5	0.86	0.10	0.04
50-5-45	0.87	0.09	0.04
50-7.5-42.5	0.85	0.12	0.03
50-10-40	0.57	0.18	0.25
50-12.5-37.5	0.25	0.21	0.54
50-15-35	0.09	0.17	0.74
50-17.5-32.5	0.05	0.21	0.74

Table 2. Lang et al.

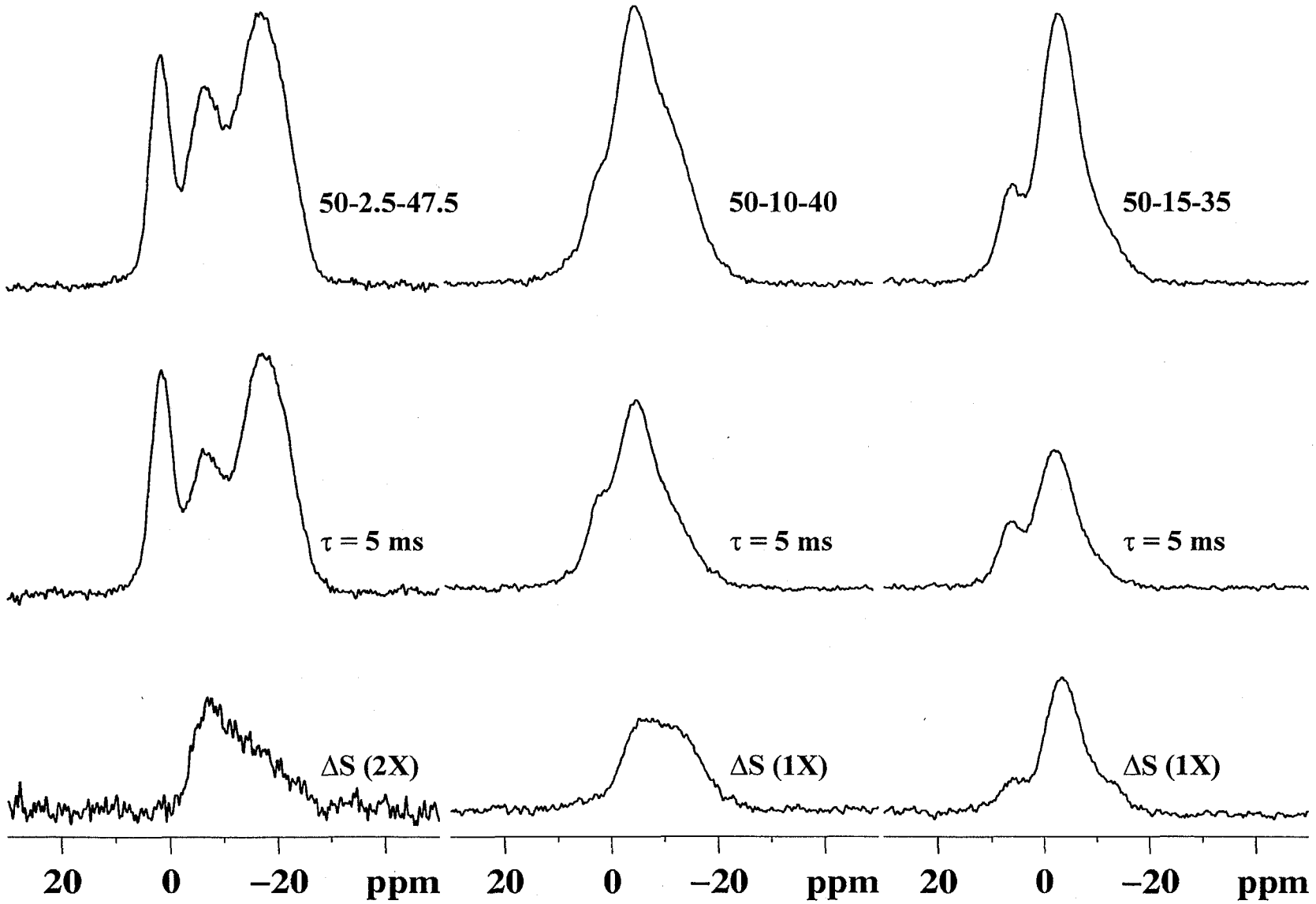

Figure 5. Lang et al.

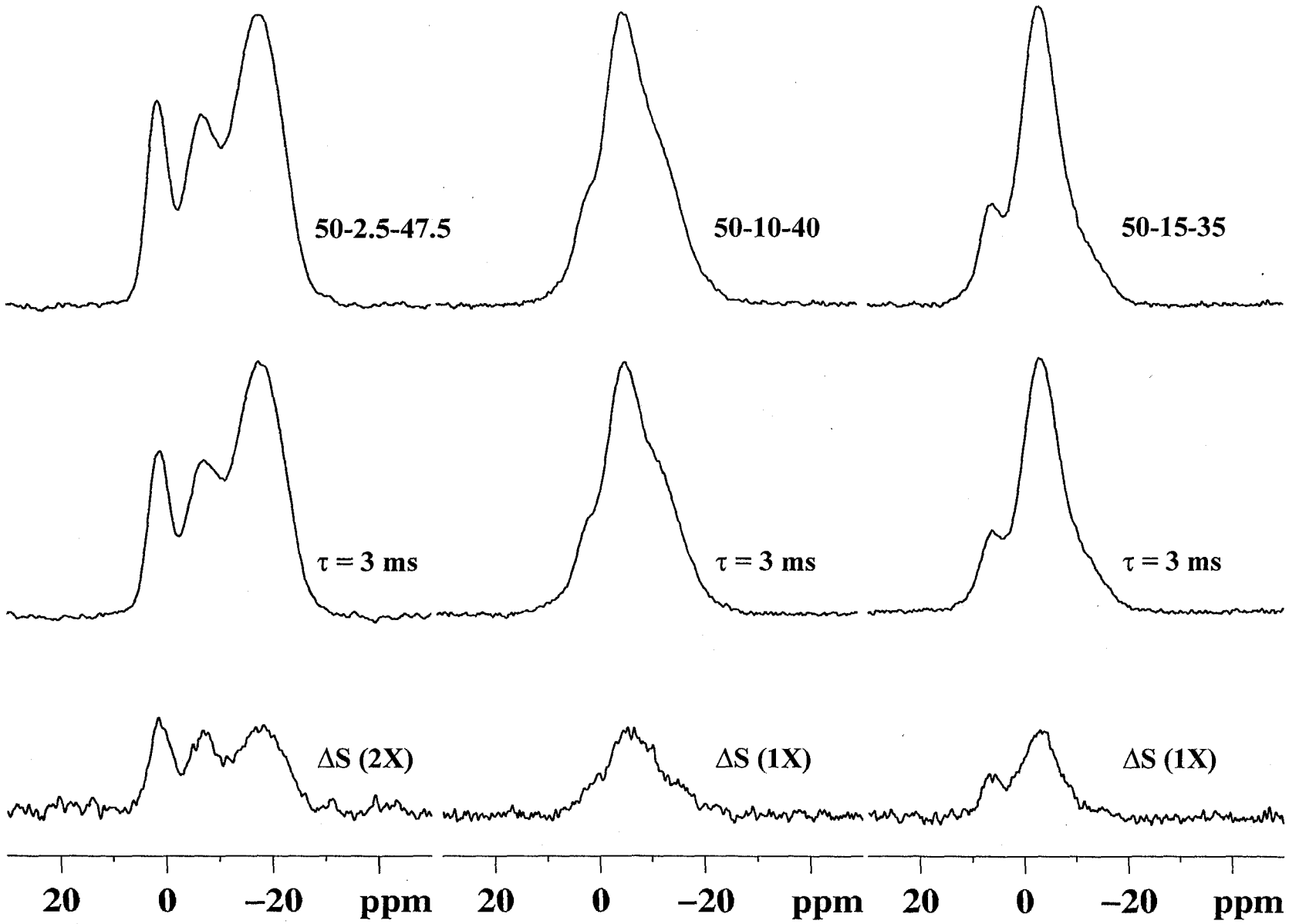

Figure 6. Lang et al.

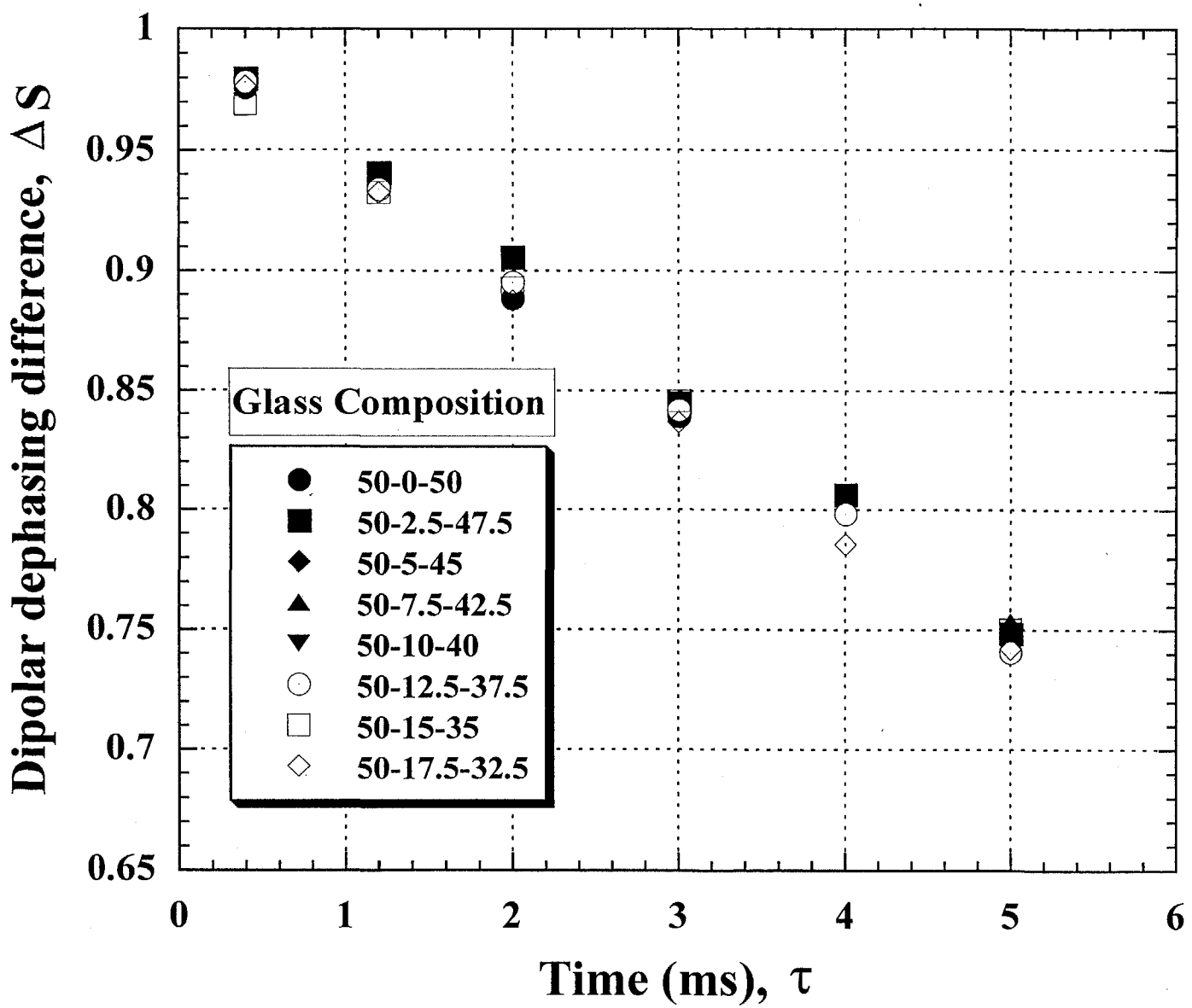

Figure 7. Lang et al.